PROCEEDINGS OF SCIENCE

Second order QCD corrections to the $g+g \to H+H$ four-point amplitude

Pulak Banerjee*
The Institute of Mathematical Sciences, HBNI, Taramani, Chennai-600113, India
E-mail: pulak.banerjee@psi.ch

Sophia Borowka
Theoretical Physics Department, CERN, CH-1211 Geneva, Switzerland
E-mail: sophia.borowka@cern.ch

Prasanna K. Dhani
The Institute of Mathematical Sciences, HBNI, Taramani, Chennai-600113, India
E-mail: prasannakd@imsc.res.in

Thomas Gehrmann
Physik-Institut, Universität Zürich, Winterthurerstrasse 190, CH-8057 Zürich, Switzerland
E-mail: thomas.gehrmann@uzh.ch

V. Ravindran
The Institute of Mathematical Sciences, HBNI, Taramani, Chennai-600113, India
E-mail: ravindra@imsc.res.in

In this contribution we compute the two loop massless QCD corrections to the four-point amplitude $g+g \to H+H$. We work in the effective theory where the Higgs boson interact with gluons in the infinite top quark mass limit. Our calculation is an important ingredient to the third-order QCD corrections to Higgs boson pair production.

14th International Symposium on Radiative Corrections (RADCOR2019)
9-13 September 2019
Palais des Papes, Avignon, France

*Speaker.

PoS(RADCOR2019)011

1. Introduction

The trilinear self coupling of the Higgs boson is a crucial parameter to describe the shape of the Higgs potential. By precisely measuring the mass of this particle, the trilinear self coupling can be accurately predicted. This coupling can be probed through the production of a pair of Higgs boson [2, 3, 4, 5]; the latter being produced dominantly at hadron colliders through the gluon fusion mechanism [6, 7]. The Standard Model (SM) production cross section of two Higgs bosons in the final state is of the order of a few tens of femtobarns at the Large Hadron Collider. This small cross section and a large irreducible background [8, 9, 10, 11, 12, 13] make it difficult and challenging to detect the final state experimentally. To determine the trilinear coupling accurately, the uncertainties in the cross sections, for two Higgs bosons in the final state, need to be under control. With the increasing accuracy of experiments, it is important to go beyond NNLO to make precise predictions for observables. Substantial progress has been made on the theoretical side in computing the higher order QCD corrections to the production of di-higgs. Since higher order corrections with exact top-quark mass dependence are difficult to compute, it is possible to restore to an effective field theoretic approach, where in the heavy-top-quark mass limit, the top quark degrees of freedom are integrated out. In this approximation, the next-to- leading order (NLO) QCD corrections has been performed in the article [2]. Subsequently the NLO calculation have been improved by considering top quark mass effects [14, 15, 16, 17, 18, 19]. Further, the full NLO calculation with exact top quark mass dependence was computed in [20, 21, 22]. At next-to-next-to-leading order (NNLO), results in the heavy top limit for soft-virtual contributions can be found in [23]; the effect of top quarks were studied in [24]; fully differential results at NNLO level can be found in [25, 26, 27]. For threshold resummation see [27, 28]. In this proceedings we compute [1] the two loop QCD corrections, in the effective theory, to a class of diagrams that is needed to compute the full three loop inclusive cross section and differential distributions for di-higgs production. In section 2 we describe the theoretical aspects and the class of diagrams that we compute. Section 3 and 4 describe the details of the computation. Numerical evaluations of the amplitude are discussed in section 5. Finally we conclude in section 6.

2. Contributions to N^{3}LO

2.1 Effective Lagrangian density

In the effective theory framework, where the top quark degrees of freedom are integrated out, the effective Lagrangian density that encodes the coupling of gluons to one and two Higgs boson is given by

$$\mathscr{L}_{eff} = -\frac{1}{4}\left(C_H(a_s)\frac{\phi}{v} - C_{HH}(a_s)\frac{\phi^2}{v^2}\right) G_{\mu\nu}G^{\mu\nu}\,, \tag{2.1}$$

where $G_{\mu\nu}$ denotes the gluon field strength tensor, ϕ, the Higgs boson and $v = 246$ GeV is the vacuum expectation value of the Higgs field. In this work we compute the relevant amplitudes for the production of two Higgs boson in the final state, described by the Lagrangian density. The constants C_H and C_{HH} denote the Wilson coefficients [29, 30, 31, 32, 33, 34]; they are determined by matching the effective theory to the full theory. Expanding in powers of the renormalized strong coupling constant $a_s = g_s^2(\mu_R^2)/(16\pi^2) = \alpha_s(\mu_R^2)/(4\pi)$ with μ_R the renormalisation scale,

$$
\begin{aligned}
C_H(a_s) &= -\frac{4a_s}{3}\Bigg[1 + a_s\Big(11\Big) + a_s^2\Bigg(\Bigg\{\frac{2777}{18} + 19L\Bigg\} + n_f\Bigg\{-\frac{67}{6} + \frac{16}{3}L\Bigg\}\Bigg) \\
&\quad + a_s^3\Bigg(-\frac{2892659}{648} + \frac{3466}{9}L + 209L^2 + \frac{897943}{144}\zeta_3 + n_f\Bigg\{\frac{40291}{324} \\
&\quad + \frac{1760}{27}L + 46L^2 - \frac{110779}{216}\zeta_3\Bigg\} + n_f^2\Bigg\{-\frac{6865}{486} + \frac{77}{27}L - \frac{32}{9}L^2\Bigg\}\Bigg)\Bigg], \qquad (2.2)\\
C_{HH}(a_s) &= -\frac{4a_s}{3}\Bigg[1 + a_s\Big(11\Big) + a_s^2\Bigg(\frac{3197}{18} + 19L + n_f\Bigg\{-\frac{1}{2} + \frac{16}{3}L\Bigg\}\Bigg)\Bigg], \qquad (2.3)
\end{aligned}
$$

In above, $L = \log\left(\frac{\mu_R^2}{m_t^2}\right)$, n_f is the number of light flavors, m_t is the $\overline{MS}$ top quark mass at scale μ_R and $N = 3$ is fixed for QCD.

2.2 Tensors and projectors

Gauge invariance allows to decompose the amplitude for the process

$$
g(p_1) + g(p_2) \to H(p_3) + H(p_4)\,, \qquad (2.4)
$$

in terms of two second rank Lorentz tensors $\mathscr{T}_i^{\mu\nu}$ with $i = 1,2$ as follows [6]:

$$
\mathscr{M}_{ab}^{\mu\nu} = \delta_{ab}\left(\mathscr{T}_1^{\mu\nu}\,\mathscr{M}_1 + \mathscr{T}_2^{\mu\nu}\,\mathscr{M}_2\right). \qquad (2.5)
$$

In eqn. (2.4), the incoming gluons carry momenta p_1 and p_2 while p_3 and p_4 are the momenta for the outgoing Higgs bosons. The Mandelstam variables for the above process are given by

$$
s = (p_1 + p_2)^2, \quad t = (p_1 - p_3)^2, \quad u = (p_2 - p_3)^2, \qquad (2.6)
$$

with $s + t + u = 2m_h^2$ where m_h is the mass of the Higgs boson. The amplitude can also be expressed in terms of the dimensionless variables x, y and z through

$$
s = m_h^2\frac{(1+x)^2}{x}, \quad t = -m_h^2 y, \quad u = -m_h^2 z. \qquad (2.7)
$$

The amplitude in eqn. (2.5) is diagonal in the color space, denoted by indices (a,b) of the incoming gluons. The Lorentz tensors are given by

$$
\begin{aligned}
\mathscr{T}_1^{\mu\nu} &= g^{\mu\nu} - \frac{1}{p_1\cdot p_2}\left(p_1^\nu p_2^\mu\right) \qquad (2.8)\\
\mathscr{T}_2^{\mu\nu} &= g^{\mu\nu} + \frac{1}{p_1\cdot p_2\; p_T^2}\left(m_h^2\,p_2^\mu p_1^\nu - 2p_1\cdot p_3\;p_2^\mu p_3^\nu - 2p_2\cdot p_3\;p_3^\mu p_1^\nu + 2p_1\cdot p_2\;p_3^\mu p_3^\nu\right), \qquad (2.9)
\end{aligned}
$$

with $p_T^2 = (tu - m_h^4)/s$. Using appropriate projectors in d dimensions

$$
\begin{aligned}
P_1^{\mu\nu} &= \frac{1}{4}\frac{d-2}{d-3}\mathscr{T}_1^{\mu\nu} - \frac{1}{4}\frac{d-4}{d-3}\mathscr{T}_2^{\mu\nu}\,,\\
P_2^{\mu\nu} &= -\frac{1}{4}\frac{d-4}{d-3}\mathscr{T}_1^{\mu\nu} + \frac{1}{4}\frac{d-2}{d-3}\mathscr{T}_2^{\mu\nu}\,, \qquad (2.10)
\end{aligned}
$$

we can obtain the scalar functions $\mathcal{M}_i$ from $\mathcal{M}_{ab}^{\mu\nu}$ as follows:

$$\mathcal{M}_i = \frac{1}{N^2-1}\, P_i^{\mu\nu}\mathcal{M}_{\mu\nu}^{ab}\delta_{ab}, \qquad i = 1,2. \tag{2.11}$$

In the next section we elaborate on the classes of diagrams that are relevant for our current work.

2.3 Classes of diagrams

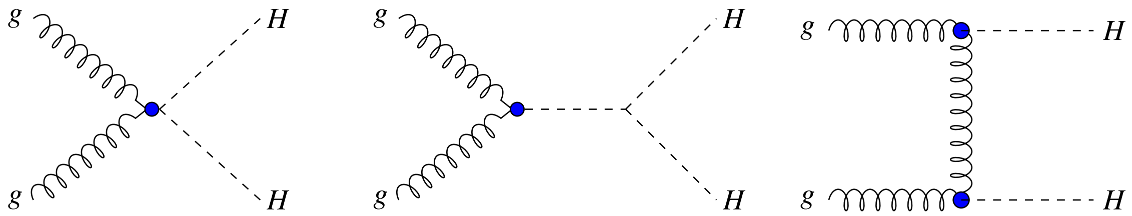

Figure 1: Class-A amplitudes (first and second diagram from left) and class-B amplitude (on the right).

Upon expanding the amplitudes $\mathcal{M}_i$ in powers of the strong coupling constant, a_s, we encounter two topologically distinct class of subprocesses. In other words, the scalar amplitudes $\mathcal{M}_i$ in eqn. (2.5) can be written as sum of amplitudes resulting from two distinct classes A and B

$$\mathcal{M}_i = \mathcal{M}_i^A + \mathcal{M}_i^B, \qquad i = 1,2. \tag{2.12}$$

where for each i, the terms on the right hand side of the above equation can be expanded in a perturbative series of a_s. The classes are as follows (see [1] for more details):

- Class-A, the first two diagrams from left in fig. 1, contains two Higgs bosons which couple to each other and to gluons. The diagrams which contain a Higgs propagator are linearly proportional to the triple Higgs coupling λ.
- Class-B, right most diagram in fig. 1, consists of Higgs bosons coupling to two gluons through the effective vertices proportional to C_H, but they do not couple to each other.

The amplitudes $\mathcal{M}_i^A$ are proportional to the Higgs boson form factor, they can be expressed as

$$\mathcal{M}_i^A = \delta_{i1}\, i\frac{s}{2}\left(C_{HH}(a_s) - C_H(a_s)\frac{6\lambda v^2}{s-m_h^2}\right)\sum_{j=0}^{\infty} a_s^j \mathcal{F}^{(j)}(d)\,, \tag{2.13}$$

Owing to the choice of tensorial basis, the amplitude $\mathcal{M}_2^A$ is zero to all orders in perturbation theory. The form factors $\mathcal{F}^{(j)}(d)$ for $j = 1,2,3$ are known in the literature [35, 36]. The class-B amplitudes result from the first term in $\mathcal{L}_{eff}$, have two powers of C_H at its leading order and start at $\mathcal{O}(a_s^2)$. Their results are available only up to $\mathcal{O}(a_s^3)$ [2]. In this article, we will complete the $\mathcal{O}(a_s^4)$ contributions to the $g+g \to H+H$ amplitude, by computing the class-B diagrams to this order, which amount to their two-loop corrections. These amplitudes are both ultraviolet (UV) and infrared (IR) divergent; we regularise them in dimensional regularisation by going to $d = 4-2\varepsilon$ dimension. We elaborate in the next two sections.

3. Ultraviolet renormalization

The unrenormalized amplitudes from class-B can be expanded in powers of the bare coupling constant $\hat{a}_s$ as

$$\hat{\mathcal{M}}_i^B = \hat{\mathcal{M}}_i^{B,(0)} + \left(\hat{a}_s \mu^{2\varepsilon} S_\varepsilon\right) \hat{\mathcal{M}}_i^{B,(1)} + \left(\hat{a}_s \mu^{2\varepsilon} S_\varepsilon\right)^2 \hat{\mathcal{M}}_i^{B,(2)} + \mathcal{O}(\hat{a}_s^3). \tag{3.1}$$

The bare strong coupling constant in the regularized theory is related to its renormalized counterpart, a_s, by

$$\begin{aligned}\hat{a}_s \mu^{2\varepsilon} S_\varepsilon &= a_s \mu_R^{2\varepsilon} Z(\mu_R^2) \\ &= a_s \mu_R^{2\varepsilon} \left[1 - a_s \left(\frac{\beta_0}{\varepsilon}\right) + a_s^2 \left(\frac{\beta_0^2}{\varepsilon^2} - \frac{\beta_1}{2\varepsilon}\right) + \mathcal{O}(a_s^3)\right].\end{aligned} \tag{3.2}$$

β_i are the QCD beta functions, $S_\varepsilon = \exp[(\ln 4\pi - \gamma)\varepsilon]$ with $\gamma \approx 0.5772...$ the Euler-Mascheroni constant.

In addition to coupling constant renormalisation, the amplitudes also require renormalisation of the effective operators appearing in the Lagrangian in eq. (2.1). We multiply the amplitudes with the overall renormalisation constant ($Z_{\mathcal{O}}$) [37, 38, 39]. In addition to the above we also need a new renormalisation constant Z_{11}^L, in a counter term proportional to $G_{\mu\nu}G^{\mu\nu}\phi\phi$ (class-A type) to renormalise the additional UV divergence resulting from amplitudes involving two $G_{\mu\nu}G^{\mu\nu}\phi$ type operators starting from 2-loop order in class-B amplitudes. The form of the renormalization constant was derived in details in [40]. Finally our UV renormalized amplitude is

$$\mathcal{M}_i^B = Z_{\mathcal{O}}^2 \hat{\mathcal{M}}_i^B + Z_{11}^L \hat{\mathcal{M}}_i^{A,(0)}\Big|_{\lambda=0}, \tag{3.3}$$

where Z_{11}^L is given by [40]

$$Z_{11}^L = a_s^2 \frac{\beta_1}{\varepsilon} + \mathcal{O}(a_s^3). \tag{3.4}$$

In the next section we discuss about the IR divergences in the amplitude $\mathcal{M}_i^B$.

4. Infrared factorization

The UV finite amplitudes still contain IR divergences, which show up as poles in the dimensional regularization parameter ε. Beyond the leading order, these amplitudes demonstrate a very rich universal structure in the IR region. It is to be noted that when combined with the real emission processes, these poles cancel. By exploiting the iterative structure of the IR singular parts in any UV renormalized amplitudes in QCD, Catani [41] predicted IR divergences for n-point two-loop amplitudes in terms of certain universal IR anomalous dimensions. These could be related [42] to the factorization and resummation properties of QCD amplitudes, and were subsequently generalized to higher loop order [43, 44]. Following [41], we obtain

$$\begin{aligned}\mathcal{M}_i^{B,(0)} &= \mathcal{M}_i^{B,(0)} \\ \mathcal{M}_i^{B,(1)} &= 2\mathbf{I}_g^{(1)}(\varepsilon)\mathcal{M}_i^{B,(0)} + \mathcal{M}_i^{B,(1),fin} \\ \mathcal{M}_i^{B,(2)} &= 4\mathbf{I}_g^{(2)}(\varepsilon)\mathcal{M}_i^{B,(0)} + 2\mathbf{I}_g^{(1)}(\varepsilon)\mathcal{M}_i^{B,(1)} + \mathcal{M}_i^{B,(2),fin}\end{aligned} \tag{4.1}$$

where $\mathbf{I}_g^{(1)}(\varepsilon)$, $\mathbf{I}_g^{(2)}(\varepsilon)$ are the IR singularity operators given by

$$\begin{aligned}\mathbf{I}_g^{(1)}(\varepsilon) &= -\frac{e^{\varepsilon\gamma}}{\Gamma(1-\varepsilon)}\left(\frac{C_A}{\varepsilon^2}+\frac{\beta_0}{2\varepsilon}\right)\left(-\frac{\mu_R^2}{s}\right)^{\varepsilon},\\ \mathbf{I}_g^{(2)}(\varepsilon) &= -\frac{1}{2}\mathbf{I}_g^{(1)}(\varepsilon)\left[\mathbf{I}_g^{(1)}(\varepsilon)+\frac{\beta_0}{\varepsilon}\right]+\frac{e^{-\varepsilon\gamma}\Gamma(1-2\varepsilon)}{\Gamma(1-\varepsilon)}\left[\frac{\beta_0}{2\varepsilon}+K\right]\mathbf{I}_g^{(1)}(2\varepsilon)+2\mathbf{H}_g^{(2)}(\varepsilon),\end{aligned} \tag{4.2}$$

with

$$\begin{aligned}K &= \left(\frac{67}{18}-\zeta_2\right)C_A-\frac{10}{9}T_F n_f,\\ \mathbf{H}_g^{(2)}(\varepsilon) &= -\left(-\frac{\mu_R^2}{s}\right)^{2\varepsilon}\frac{e^{\varepsilon\gamma}}{\Gamma(1-\varepsilon)}\\ &\quad\times\frac{1}{2\varepsilon}\left\{C_A^2\left(-\frac{5}{24}-\frac{11}{48}\zeta_2-\frac{1}{4}\zeta_3\right)+C_A n_f\left(\frac{29}{54}+\frac{1}{24}\zeta_2\right)-\frac{1}{4}C_F n_f-\frac{5}{54}n_f^2\right\}.\end{aligned} \tag{4.3}$$

where the SU(N) color factors $C_A = N$, $C_F = \frac{N^2-1}{2N}$, and $T_F = \frac{1}{2}$. Our amplitudes show the correct universal infrared behaviour, which is a stringent check on our results.

5. Computation and results

The Feynman diagrams for class-B were generated using QGRAF. This output was then exported to FORM to perform all the algebraic manipulations, which includes Lorentz, Dirac and color algebra; the final output is expressed in terms of several Feynman integrals. These integrals are then reduced to few set of master integrals, using two independent packages LiteRed [45] and REDUZE2 [46, 47] . Using the analytical form of the master integrals which were computed in the works [48, 49], we get the unrenormalized amplitudes $\hat{\mathscr{M}}_i^{B,(1)}$ and $\hat{\mathscr{M}}_i^{B,(2)}$. See [1] for more details. In section 3 and 4 we described in details the UV renomalization of the amplitudes and then checking their IR singularities. The finite remainders $\mathscr{M}_i^{B,(j),fin}$, $i = 1,2$ (in eqn. (4.1) contain multiple classical polylogarithms which are functions of the scaling variables x, y and their coefficients further depend on the Higgs mass m_h. In the centre of mass frame, we plot the real and imaginary parts of the two-loop finite remainders after expressing the scaling variables as function of s, m_h^2 and $\cos(\theta)$, where θ is the angle between one of the Higgs bosons in the final state and one of the initial gluons. In addition, we set $m_h = 125$ GeV with $\mu_R^2 = m_h^2/2$ and extract an additional factor of m_h^2 in the plots. Being a purely bosonic amplitude, $\mathscr{M}_i^{B,(j),fin}|_{\cos(\theta)\to-\cos(\theta)} = \mathscr{M}_i^{B,(j),fin}$. This symmetry serves as a strong check on our results. In the left panel of fig. 2, we display the real and imaginary parts of the amplitude $\mathscr{M}_1^{B,(2),fin}$; for $\mathscr{M}_2^{B,(2),fin}$, see the right panel. The insets show the behaviour of the amplitudes close to the boundary of physical region, $x = 0$. We observe stable behaviour of the finite parts of our two-loop amplitude.

6. Conclusion

We compute the two-loop massless QCD corrections to the $g+g\to H+H$ amplitude, which is the last missing piece required for the full computation of N^{3}LO corrections to Higgs boson pair

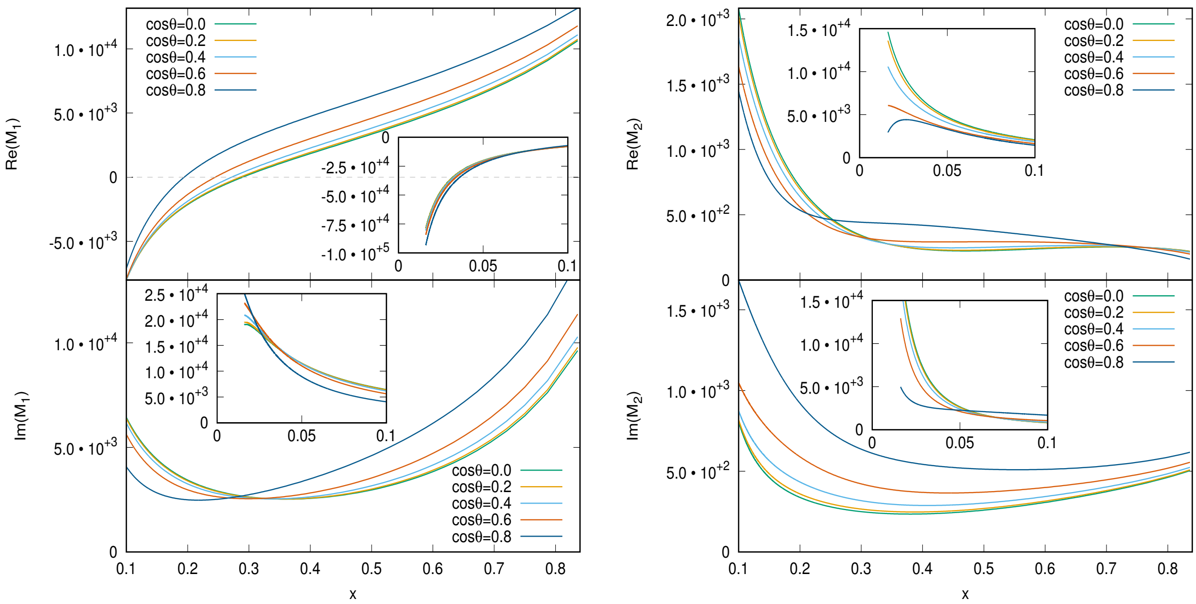

Figure 2: Behavior of $\mathcal{M}_1^{B,(2),fin}$ (left) and $\mathcal{M}_2^{B,(2),fin}$ (right) as a function of the scaling variable x for different values of $\cos(\theta)$. The insets show the region close to $x = 0$.

production in gluon fusion [58], in the infinite top quark mass limit. We saw that in the effective theory there are two classes of diagrams that gives rise to two Higgs final state. The three loop QCD corrections are already known for class-A, the one loop amplitudes for class-B have been known for a while in the effective theory. Although an exact calculation is currently out of reach, reweighting procedures allows to reliably quantify these effects [59]. Our newly computed amplitudes will be useful for computing the hard matching coefficients in the resummation of corrections at low pair transverse momentum. To compute differential distributions of the Higgs boson pair production, proper techniques are needed to handle the IR singular real radiation; the first steps have been taken in [60, 61]. Our calculation opens up possibilities for more precise phenomenological predictions in Higgs boson pair production at the hadron colliders.

References

[1] Pulak Banerjee, Sophia Borowka, Prasanna K. Dhani, Thomas Gehrmann and V. Ravindran, *Two-loop massless QCD corrections to the $g+g \to H+H$ four-point amplitude*, *JHEP* **11** (2018) 130, [1809.05388].

[2] S. Dawson, S. Dittmaier and M. Spira, *Neutral Higgs boson pair production at hadron colliders: QCD corrections*, *Phys. Rev.* **D58** (1998) 115012, [hep-ph/9805244].

[3] A. Djouadi, W. Kilian, M. Mühlleitner and P. M. Zerwas, *Testing Higgs selfcouplings at e^+e^- linear colliders*, *Eur. Phys. J.* **C10** (1999) 27–43, [hep-ph/9903229].

[4] A. Djouadi, W. Kilian, M. Mühlleitner and P. M. Zerwas, *Production of neutral Higgs boson pairs at LHC*, *Eur. Phys. J.* **C10** (1999) 45–49, [hep-ph/9904287].

[5] M. M. Mühlleitner, *Higgs particles in the standard model and supersymmetric theories*, Ph.D. thesis, Hamburg U., 2000. hep-ph/0008127.

[6] E. W. N. Glover and J. J. van der Bij, *Higgs boson pair production via gluon fusion*, Nucl. Phys. **B309** (1988) 282–294.

[7] T. Plehn, M. Spira and P. M. Zerwas, *Pair production of neutral Higgs particles in gluon-gluon collisions*, Nucl. Phys. **B479** (1996) 46–64, [hep-ph/9603205].

[8] J. Baglio, A. Djouadi, R. Gröber, M. M. Mühlleitner, J. Quevillon and M. Spira, *The measurement of the Higgs self-coupling at the LHC: theoretical status*, JHEP **04** (2013) 151, [1212.5581].

[9] V. Barger, L. L. Everett, C. B. Jackson and G. Shaughnessy, *Higgs-Pair Production and Measurement of the Triscalar Coupling at LHC(8,14)*, Phys. Lett. **B728** (2014) 433–436, [1311.2931].

[10] M. J. Dolan, C. Englert and M. Spannowsky, *Higgs self-coupling measurements at the LHC*, JHEP **10** (2012) 112, [1206.5001].

[11] A. Papaefstathiou, L. L. Yang and J. Zurita, *Higgs boson pair production at the LHC in the $b\bar{b}W^+W^-$ channel*, Phys. Rev. **D87** (2013) 011301, [1209.1489].

[12] D. E. Ferreira de Lima, A. Papaefstathiou and M. Spannowsky, *Standard model Higgs boson pair production in the $(b\bar{b})(b\bar{b})$ final state*, JHEP **08** (2014) 030, [1404.7139].

[13] J. K. Behr, D. Bortoletto, J. A. Frost, N. P. Hartland, C. Issever and J. Rojo, *Boosting Higgs pair production in the $b\bar{b}b\bar{b}$ final state with multivariate techniques*, Eur. Phys. J. **C76** (2016) 386, [1512.08928].

[14] J. Grigo, J. Hoff, K. Melnikov and M. Steinhauser, *On the Higgs boson pair production at the LHC*, Nucl. Phys. **B875** (2013) 1–17, [1305.7340].

[15] R. Frederix, S. Frixione, V. Hirschi, F. Maltoni, O. Mattelaer, P. Torrielli, E. Vryonidou and M. Zaro, *Higgs pair production at the LHC with NLO and parton-shower effects*, Phys. Lett. **B732** (2014) 142–149, [1401.7340].

[16] F. Maltoni, E. Vryonidou and M. Zaro, *Top-quark mass effects in double and triple Higgs production in gluon-gluon fusion at NLO*, JHEP **11** (2014) 079, [1408.6542].

[17] G. Degrassi, P. P. Giardino and R. Gröber, *On the two-loop virtual QCD corrections to Higgs boson pair production in the Standard Model*, Eur. Phys. J. **C76** (2016) 411, [1603.00385].

[18] R. Gröber, A. Maier and T. Rauh, *Reconstruction of top-quark mass effects in Higgs pair production and other gluon-fusion processes*, JHEP **03** (2018) 020, [1709.07799].

[19] R. Bonciani, G. Degrassi, P. P. Giardino and R. Gröber, *Analytical Method for Next-to-Leading-Order QCD Corrections to Double-Higgs Production*, Phys. Rev. Lett. **121** (2018) 162003, [1806.11564].

[20] S. Borowka, N. Greiner, G. Heinrich, S. Jones, M. Kerner, J. Schlenk, U. Schubert and T. Zirke, *Higgs Boson Pair Production in Gluon Fusion at Next-to-Leading Order with Full Top-Quark Mass Dependence*, Phys. Rev. Lett. **117** (2016) 012001, [1604.06447].

[21] S. Borowka, N. Greiner, G. Heinrich, S. P. Jones, M. Kerner, J. Schlenk and T. Zirke, *Full top quark mass dependence in Higgs boson pair production at NLO*, JHEP **10** (2016) 107, [1608.04798].

[22] Julien Baglio, Francisco Campanario, Seraina Glaus, Margarete Mühlleitner, Michael Spira, Juraj Streicher, *Gluon fusion into Higgs pairs at NLO QCD and the top mass scheme*, Eur. Phys. J **10** (2019),

[23] D. de Florian and J. Mazzitelli, *Two-loop virtual corrections to Higgs pair production*, *Phys. Lett.* **B724** (2013) 306–309, [1305.5206].

[24] J. Grigo, J. Hoff and M. Steinhauser, *Higgs boson pair production: top quark mass effects at NLO and NNLO*, *Nucl. Phys.* **B900** (2015) 412–430, [1508.00909].

[25] Q. Li, Q.-S. Yan and X. Zhao, *Higgs Pair Production: Improved Description by Matrix Element Matching*, *Phys. Rev.* **D89** (2014) 033015, [1312.3830].

[26] P. Maierhöfer and A. Papaefstathiou, *Higgs Boson pair production merged to one jet*, *JHEP* **03** (2014) 126, [1401.0007].

[27] D. de Florian and J. Mazzitelli, *Higgs pair production at next-to-next-to-leading logarithmic accuracy at the LHC*, *JHEP* **09** (2015) 053, [1505.07122].

[28] D. Y. Shao, C. S. Li, H. T. Li and J. Wang, *Threshold resummation effects in Higgs boson pair production at the LHC*, *JHEP* **07** (2013) 169, [1301.1245].

[29] J. Grigo, K. Melnikov and M. Steinhauser, *Virtual corrections to Higgs boson pair production in the large top quark mass limit*, *Nucl. Phys.* **B888** (2014) 17–29, [1408.2422].

[30] A. Djouadi, M. Spira and P. M. Zerwas, *Production of Higgs bosons in proton colliders: QCD corrections*, *Phys. Lett.* **B264** (1991) 440–446.

[31] M. Kramer, E. Laenen and M. Spira, *Soft gluon radiation in Higgs boson production at the LHC*, *Nucl. Phys.* **B511** (1998) 523–549, [hep-ph/9611272].

[32] K. G. Chetyrkin, B. A. Kniehl and M. Steinhauser, *Hadronic Higgs decay to order* α_s^4, *Phys. Rev. Lett.* **79** (1997) 353–356, [hep-ph/9705240].

[33] M. Spira, *Effective Multi-Higgs Couplings to Gluons*, *JHEP* **10** (2016) 026, [1607.05548].

[34] M. Gerlach, F. Herren and M. Steinhauser, *Wilson coefficients for Higgs boson production and decoupling relations to* $\mathcal{O}\left(\alpha_s^4\right)$, *JHEP* **1811 (2018) 141** , 1809.06787.

[35] P. A. Baikov, K. G. Chetyrkin, A. V. Smirnov, V. A. Smirnov and M. Steinhauser, *Quark and gluon form factors to three loops*, *Phys. Rev. Lett.* **102** (2009) 212002, [0902.3519].

[36] T. Gehrmann, E. W. N. Glover, T. Huber, N. Ikizlerli and C. Studerus, *Calculation of the quark and gluon form factors to three loops in QCD*, *JHEP* **06** (2010) 094, [1004.3653].

[37] N. K. Nielsen, *Gauge Invariance and Broken Conformal Symmetry*, *Nucl. Phys.* **B97** (1975) 527–540.

[38] V. P. Spiridonov and K. G. Chetyrkin, *Nonleading mass corrections and renormalization of the operators* $m\bar{\psi}\psi$ *and* $G^2_{\mu\nu}$, *Sov. J. Nucl. Phys.* **47** (1988) 522–527.

[39] A. L. Kataev, N. V. Krasnikov and A. A. Pivovarov, *Two Loop Calculations for the Propagators of Gluonic Currents*, *Nucl. Phys.* **B198** (1982) 508–518, [hep-ph/9612326].

[40] M. F. Zoller, *On the renormalization of operator products: the scalar gluonic case*, *JHEP* **04** (2016) 165, [1601.08094].

[41] S. Catani, *The Singular behavior of QCD amplitudes at two loop order*, *Phys. Lett.* **B427** (1998) 161–171, [hep-ph/9802439].

[42] G. F. Sterman and M. E. Tejeda-Yeomans, *Multiloop amplitudes and resummation*, *Phys. Lett.* **B552** (2003) 48–56, [hep-ph/0210130].

[43] T. Becher and M. Neubert, *Infrared singularities of scattering amplitudes in perturbative QCD*, *Phys. Rev. Lett.* **102** (2009) 162001, [0901.0722].

[44] E. Gardi and L. Magnea, *Factorization constraints for soft anomalous dimensions in QCD scattering amplitudes*, *JHEP* **03** (2009) 079, [0901.1091].

[45] R. N. Lee, *LiteRed 1.4: a powerful tool for reduction of multiloop integrals*, *J. Phys. Conf. Ser.* **523** (2014) 012059, [1310.1145].

[46] C. Studerus, *Reduze-Feynman Integral Reduction in C++*, *Comput. Phys. Commun.* **181** (2010) 1293–1300, [0912.2546].

[47] A. von Manteuffel and C. Studerus, *Reduze 2 - Distributed Feynman Integral Reduction*, 1201.4330.

[48] T. Gehrmann, A. von Manteuffel, L. Tancredi and E. Weihs, *The two-loop master integrals for* $q\bar{q} \to VV$, *JHEP* **06** (2014) 032, [1404.4853].

[49] T. Gehrmann, L. Tancredi and E. Weihs, *Two-loop master integrals for* $q\bar{q} \to VV$*: the planar topologies*, *JHEP* **08** (2013) 070, [1306.6344].

[50] F. V. Tkachov, *A Theorem on Analytical Calculability of Four Loop Renormalization Group Functions*, *Phys. Lett.* **100B** (1981) 65–68.

[51] K. G. Chetyrkin and F. V. Tkachov, *Integration by Parts: The Algorithm to Calculate beta Functions in 4 Loops*, *Nucl. Phys.* **B192** (1981) 159–204.

[52] T. Gehrmann and E. Remiddi, *Differential equations for two loop four point functions*, *Nucl. Phys.* **B580** (2000) 485–518, [hep-ph/9912329].

[53] S. Laporta, *High precision calculation of multiloop Feynman integrals by difference equations*, *Int. J. Mod. Phys.* **A15** (2000) 5087–5159, [hep-ph/0102033].

[54] C. Anastasiou and A. Lazopoulos, *Automatic integral reduction for higher order perturbative calculations*, *JHEP* **07** (2004) 046, [hep-ph/0404258].

[55] A. V. Smirnov, *Algorithm FIRE – Feynman Integral REduction*, *JHEP* **10** (2008) 107, [0807.3243].

[56] C. Anastasiou, C. Duhr, F. Dulat, F. Herzog and B. Mistlberger, *Higgs Boson Gluon-Fusion Production in QCD at Three Loops*, *Phys. Rev. Lett.* **114** (2015) 212001, [1503.06056].

[57] B. Mistlberger, *Higgs boson production at hadron colliders at* N^3LO *in QCD*, *JHEP* **05** (2018) 028, [1802.00833].

[58] Long-Bin Chen, Hai Tao Li, Hua-Sheng Shao and Jian Wang, *Higgs boson pair production via gluon fusion at* N^3LO *in QCD*, [1909.06808].

[59] M. Grazzini, G. Heinrich, S. Jones, S. Kallweit, M. Kerner, J. M. Lindert and J. Mazzitelli, *Higgs boson pair production at NNLO with top quark mass effects*, *JHEP* **05** (2018) 059, [1803.02463].

[60] J. Currie, T. Gehrmann, E. W. N. Glover, A. Huss, J. Niehues and A. Vogt, N^3LO *corrections to jet production in deep inelastic scattering using the Projection-to-Born method*, *JHEP* **05** (2018) 209, [1803.09973].

[61] L. Cieri, X. Chen, T. Gehrmann, E. W. N. Glover and A. Huss, *Higgs boson production at the LHC using the* q_T *subtraction formalism at* N^3LO *QCD*, *JHEP* **1902 (2019) 096**, [1807.11501].